

A green slow-release fertilizer composition based on urea-modified hydroxyapatite nanoparticles encapsulated wood

Nilwala Kottegoda*, Imalka Munaweera, Nadeesh Madusanka and Veranja Karunaratne

Sri Lanka Institute of Nanotechnology,
Biyagama Export Processing Zone, Colombo, Sri Lanka

In this paper we describe a strategy for sustained release of nitrogen into the soil. Specifically, urea-modified hydroxyapatite nanoparticles were encapsulated under pressure into cavities of the soft wood of *Gliricidia sepium*. Nitrogen release of the nanofertilizer composition was studied using soil from three elevations in Sri Lanka (pH 4.2, 5.2 and 7) and compared with that of a commercial fertilizer. The nanofertilizer showed an initial burst and a subsequent slow-release even on day 60 compared to the commercial fertilizer, which released heavily early followed by the release of low and non-uniform quantities until around day 30.

Keywords: Fertilizer, macronutrients, slow-release, nanoparticles, wood stem.

EVALUATED as a key nutrient source for food, fibre and biomass production in agriculture, nitrogen is the most important element in fertilizers. However, considering the energy required in its synthesis and the large tonnage required, the nitrogen fertilizer has a high monetary value. Because 50–70% of the nitrogen applied using conventional fertilizers, with particle size dimensions greater than 100 nm, is lost to the soil due to leaching, nitrogen utilization efficiency (NUE) by plants is low, adding to the cost of getting nitrogen into the plant; leaching of nitrogen can happen by way of water-soluble nitrates, emission as ammonia and nitrogen oxides, and soil microorganism-mediated incorporation into soil organic matter over time¹. Attempts to increase the NUE in conventional fertilizer formulations have thus far resulted in little success. On the other hand, the emerging nanostrategies indicate that, due to the high surface area to volume ratio, nanofertilizers are expected to be far more effective than even polymer-coated conventional slow-release fertilizers^{2–5}. In this backdrop, we report here a nanostrategy involving a slow-release fertilizer composition based on urea-modified hydroxyapatite (HA) nanoparticles encapsulated into the cavities present in soft wood.

HA ($\text{Ca}_{10}(\text{PO}_4)_6(\text{OH})_2$) nanoparticles are rated as one of the prominent candidates in agricultural applications, which can provide phosphorus nutrient. Much of the cur-

rent literature on HA is however focused on its biomedical applications^{6–12} due to its excellent biocompatibility and bioactivity, while potential agricultural applications have not been adequately addressed. Several research groups have adapted different methods to synthesize HA nanoparticles, such as wet chemical precipitation^{13–17}, hydrothermal method^{18–20}, sol-gel method²¹ and spray pyrolysis process²². Morphology and the level of the crystallinity of the nanoparticles highly depend on the preparation method and the experimental conditions. Wet chemical precipitation of HA nanoparticles is the simplest available method for the synthesis with a high yield. HA nanoparticles were also envisaged as a suitable candidate for ready surface modification with different organic and inorganic materials due to their rich surface chemistry, and several applications have been recorded in the literature. Many research groups have attempted to synthesize chitosan-nanohydroxyapatite composites, especially for tissue engineering applications^{23–25}, biodegradable and biocompatible nanohydroxyapatite polyvinyl alcohol composites²⁶, and amino acid-functionalized hydroxyapatite nanorods, to be used as building blocks for the preparation of bioinorganic nanocomposites²⁷.

In our study, HA nanoparticles were synthesized by wet chemical methods¹³ and surface modified with urea, the most widely used water-soluble plant nitrogen nutrient source, and a fertilizer composition was manufactured by encapsulation of urea-modified HA nanoparticles into micro/nano porous cavities of the young stem of *Gliricidia sepium* (Jacq.) Kunth Walp., under pressure. These cavities are defined by cellular polymers such as cellulose, hemi-cellulose and lignin. Then the resulting bio-nanocomposite was dried and used in pellet form. It was hypothesized that once this nanofertilizer composition contained in a superabsorbent biopolymeric matrix is incorporated into a soil system, it will absorb moisture, thus initiating slow and sustained release of nitrogen into the soil as a result of diffusion and microbial degradation.

All reagents and chemicals used in this study were purchased from Sigma (USA) and were of analytical grade and used without further purification. All solutions were prepared using distilled water.

Powder X-ray diffraction (PXRD) patterns of all synthesized samples were recorded using a Bruker D8 Focus X-ray powder diffractometer at the Sri Lanka Institute of Nanotechnology using CuK_α radiation ($\lambda = 0.154 \text{ nm}$) over a 2θ range of 3–60°, with a step size of 0.02° and a step time of 1 s. The particle size and morphology of the synthesized samples were studied using a scanning electron microscopy (SEM; HITACHI SU6600 microscope). The chemical nature and molecular bonding of the synthesized samples were studied using Fourier Transform Infra Red Spectroscopy (FTIR; Bruker Vertex80), a range from 600 to 4000 cm^{-1} using attenuated total reflectance (ATR) technique. Particle size distribution and zeta

*For correspondence. (e-mail: nilwalak@susnanotec.lk)

potential of the prepared nanodispersions were measured using Malvern Zetasizer analyzer nano ZS.

N and P contents of the prepared solid nanofertilizer compositions were analysed using Kjeldhal method and vanadomolybdate method respectively, according to SLS standards 645. Ca content was measured using atomic absorption spectroscopy. Nitrogen content of the leached samples was analysed using Kjeldhal method, according to SLS standards 645.

HA nanoparticles were synthesized as described by Mateus *et al.*¹³ using aqueous solutions of calcium hydroxide ($\text{Ca}(\text{OH})_2$) and orthophosphoric acid (H_3PO_4), 85%. In this experiment Ca:P molar ratio was maintained at 1.67. First, 0.6 M H_3PO_4 (250 ml) was added drop-wise into a suspension of calcium hydroxide (19.29 g $\text{Ca}(\text{OH})_2$ in 250 ml water), while stirring vigorously under mechanical agitation (1000 rpm).

The reaction takes place according to the following equation.



HA nanoparticles synthesized as described above were allowed to settle and the supernatant was decanted. The resulting HA nanoparticles were washed thrice with distilled water. The solid thus obtained was dried at 100°C for 2 h. The product was characterized using PXRD, SEM and FTIR.

HA nanoparticles (25 g) synthesized as described above were dispersed in distilled water (100 ml) under ultrasonic mixing (30 kHz for 45 min). The resulting HA nanoparticle dispersion was stirred in a saturated urea solution (100 ml) at 25°C for 12 h. The resulting dispersion was allowed to settle and the excess liquid was decanted. The product was washed with distilled water to remove excess urea, and dried at 50°C for 7 h. Urea-modified HA nanoparticles were characterized using PXRD, SEM and FTIR.

Urea-modified HA nanoparticles (5 g) and sodium hexametaphosphate (2 g) were dispersed in distilled water (300 ml) under ultrasonic mixing (30 kHz for 15 min). The stability and particle size distribution of the resulting dispersion were measured using Malvern Zetasizer particle size analyser.

G. sepium stems (approximately 3–5 cm diameter) were cut into pieces of approximately 1 inch in length and further cut into 0.5 cm × 0.5 cm × 0.5 cm wood chips. Wet wood chips (15 g) were soaked in the above prepared dispersion (100 ml) and placed in a chamber which can be pressurized up to 10 bar. Different trials were carried out at 3, 5, 7, 9 and 10 bar respectively for 2 h to determine the optimum pressure in order to get maximum loading of nitrogen in cell cavities.

Soil from three elevations in Sri Lanka: sandy soil (pH 7) at sea level, acidic soil (pH 4.2) at 4000 ft and acidic soil (pH 5.2) at 1600 ft were used. First, each of the soil

samples (400 g) was mixed with a commercial fertilizer composition for tea, T65 (8 g) containing 11% N as granular ammonium sulphate purchased from Hayleys Agro Ltd, Sri Lanka. Second, urea-modified HA nanoparticle-encapsulated *G. sepium* nanofertilizer composition (weight adjusted to contain an equal amount of nitrogen as the commercial fertilizer) in pellet form was mixed separately with the three types of soil. These soil samples were filled into 500 ml separatory funnels. Next, 180 ml water was added to all six soil columns until they reached the soil–water saturation point. The moisture content in the columns was maintained approximately constant throughout the period of study by adding water (100 ml). The water in the soil was allowed to elute in five-day intervals and the eluted solution (50 ml) was collected. The nitrogen content in the eluted solutions was tested in order to study the release behaviour of the fertilizer system.

HA nanoparticles and urea-modified HA nanoparticles were characterized using a number of techniques. The PXRD pattern (Figure 1a) of HA nanoparticles is in good agreement with that reported in the powder diffraction file for HA in the ICDD, (PDF No. 09-0432).

PXRD pattern of the urea-modified HA nanoparticles (Figure 1b) indicated the presence of peaks due to HA nanoparticles. In addition, a peak corresponding to urea was observed (denoted as * in Figure 1b). Persistence of this peak even after thorough washing of the nanosystem, indicated strong interaction between urea and HA nanoparticles.

SEM images of HA nanoparticles (Figure 2a), exhibited typical rod-like morphology, with a diameter less than 100 nm and an average length of 150 nm. Significantly, urea modification of the HA nanoparticles had retained the same morphology (Figure 2b). Elemental

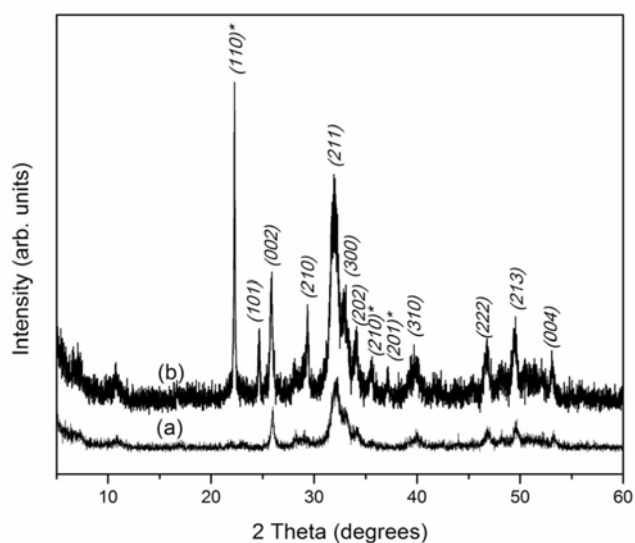
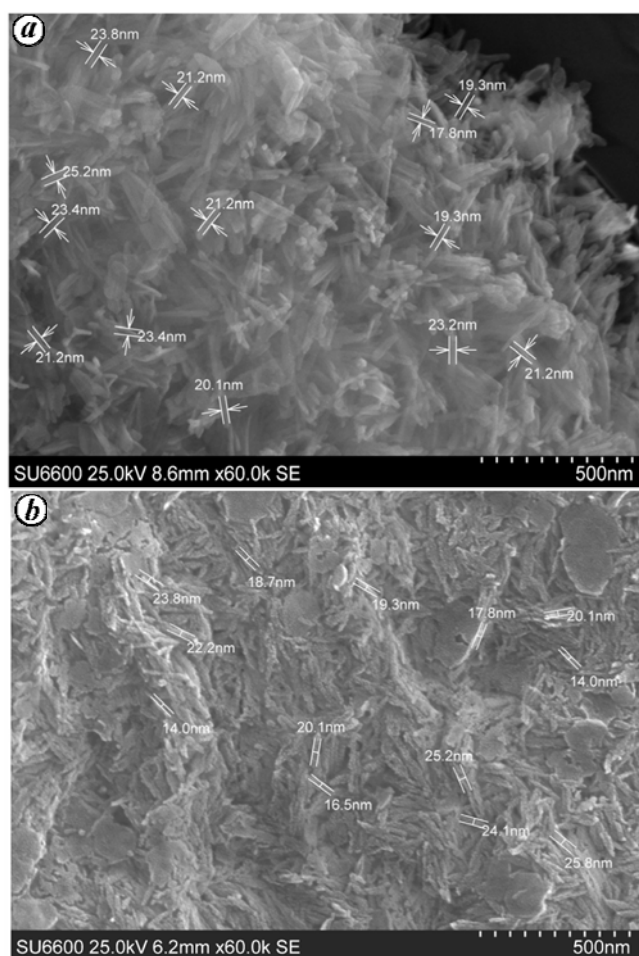


Figure 1. Powder X-ray diffraction pattern of (a) synthesized hydroxyapatite (HA) nanoparticles and (b) urea surface-modified HA nanoparticles. (* denotes the diffraction peaks due to urea.)

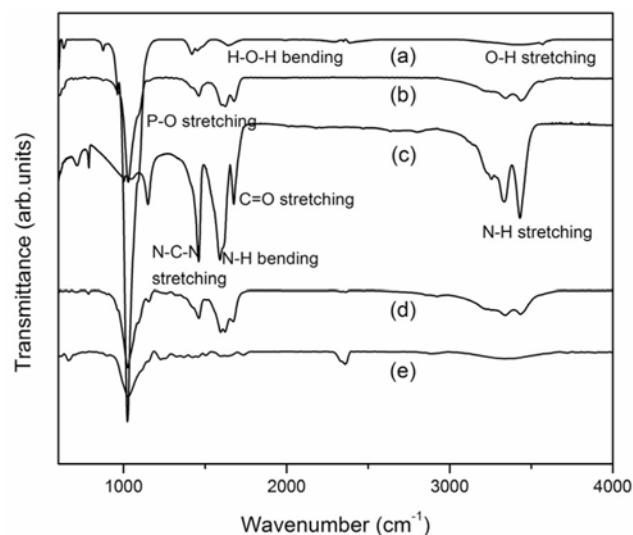
Table 1. Elemental compositions of hydroxyapatite (HA) nanoparticles, urea-modified HA nanoparticles, raw *Gliricidia sepium* and urea-modified HA nanoparticle-encapsulated *G. sepium*

Element (%)	HA nanoparticles	Urea surface-modified HA nanoparticles	Raw <i>G. sepium</i>	Urea surface-modified HA nanoparticle encapsulated <i>G. sepium</i>
N	–	33.2	1.3	14
P	17.5	6.2	0.3	3
Ca	36.8	13	0.2	1

**Figure 2.** Scanning electron microscope images of (a) synthesized HA nanoparticles and (b) urea surface-modified HA nanoparticles.

analysis further confirmed the presence of urea on HA nanoparticles (Table 1).

The FTIR spectrum (Figure 3a) further confirmed the successful synthesis of HA nanoparticles. The most prominent sharp and intense absorption band located around $\gamma_{\max}/\text{cm}^{-1}$ 1050 represents the γ_1 mode of symmetric P–O stretching vibrations of PO_4^{3-} ions in hydroxyapatite. The broad absorption band centred around $\gamma_{\max}/\text{cm}^{-1}$ 3500 confirmed the presence of hydroxyl groups. The HA bonding environment of urea-modified HA nanoparticles was clearly discerned by FTIR spectroscopy (Figure 3b)

**Figure 3.** Fourier transform infrared spectra of (a) synthesized HA nanoparticles, (b) urea-modified HA nanoparticles, (c) urea, (d) urea-modified HA nanoparticle-encapsulated *Gliricidia sepium* and (e) untreated *G. sepium*.

with the presence of the γ_1 mode described above. In addition, the N–H stretching frequency of pure urea appeared as a doublet at $\gamma_{\max}/\text{cm}^{-1}$ 3430 and 3340, which in urea bonded to HA nanoparticles was shifted to $\gamma_{\max}/\text{cm}^{-1}$ 3200, where noticeable peak broadening had occurred. This suggests significant hydrogen bonding between N–H groups of urea with O–H groups of HA nanoparticles. Although the band for the N–H bending motion of urea had shifted from $\gamma_{\max}/\text{cm}^{-1}$ 1590 to $\gamma_{\max}/\text{cm}^{-1}$ 1627 after the surface modification process, it was a clear indication of the presence of free N–H bonds even after adsorption of urea onto HA nanoparticles. The change in the carbonyl stretching frequency of pure urea from $\gamma_{\max}/\text{cm}^{-1}$ 1680 to $\gamma_{\max}/\text{cm}^{-1}$ 1656 in urea-adsorbed HA nanoparticles indicated that, as is expected, the C=O electron density was being affected by the N–H hydrogen bonding to HA. This observation was lent further credence by a noticeable peak shift of the N–C–N stretching frequency ($\gamma_{\max}/\text{cm}^{-1}$ 1460) of urea to a lower frequency in urea-modified HA nanoparticles ($\gamma_{\max}/\text{cm}^{-1}$ 1446). Thus, FTIR data established that urea is adsorbed on the surface of HA nanoparticles through several binding modes of unequal binding strengths. The schematic rep-

resentation of a possible model of the urea-modified HA nanoparticles is given in Figure 4. Having synthesized the urea-modified HA nanofertilizer system in short order, the soft wood *G. sepium* was chosen to encapsulate it. *G. sepium* is an easily propagated fast-growing legume whose young and abundant branches are about 2–3 m long with a diameter of 3–5 cm. As evidenced by the SEM image (Figure 5) of a cross-section of *G. sepium*, three types of cavities can be identified.

The size of the vascular canals can range from 1 to 30 μm , whereas the cell cavities of the plant stem vary in submicron sizes up to about 10 μm . There are intercellular spaces whose dimensions are below 100 nm.

The quality of the nanodispersion was studied prior to encapsulation by particle size analysis and zeta potential

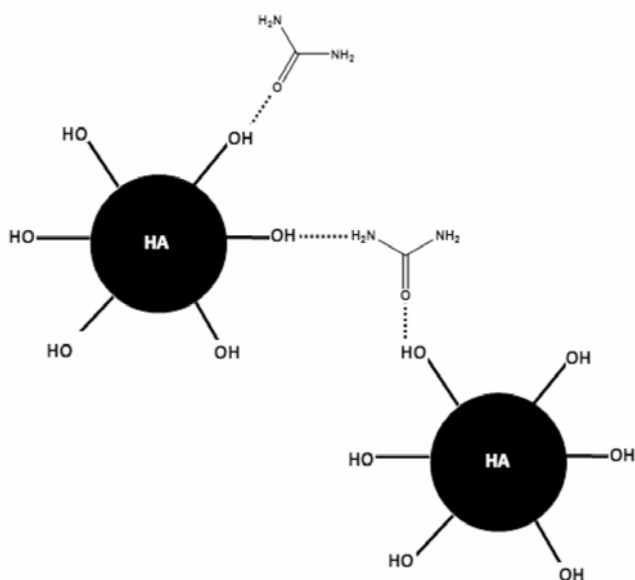


Figure 4. Schematic representation of the model for urea-modified HA nanoparticles.

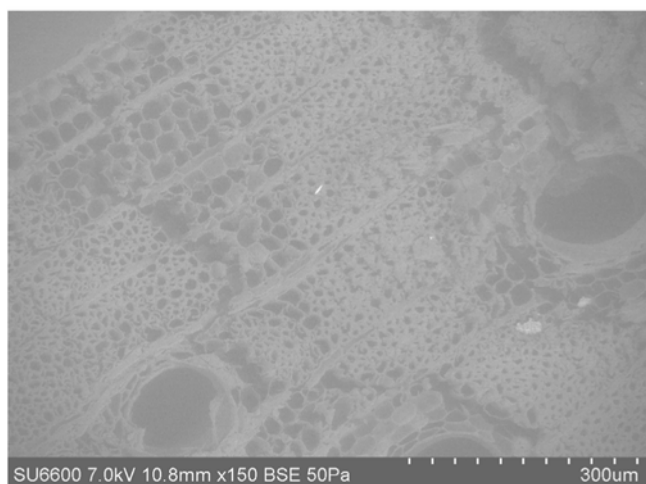


Figure 5. SEM image of *G. sepium* stem.

measurements. It was observed that the size of majority of the particles in the dispersion was below 100 nm (size-averaged particle size) and zeta potential was -56.9 mV, confirming the presence of a stable nanodispersion.

The optimum pressure required to achieve the maximum loading of N is about 9 bar and above this pressure the impregnated N percentage is very low compared with the results at low pressure (Figure 6). At high pressure, the destruction of cell cavities and cell walls may be the reason for the low loadings. The random elemental composition of urea-modified HA nanoparticle-encapsulated *G. sepium* chips confirmed the presence of added nitrogen by comparison with the NPK analysis of untreated *G. sepium*. Table 1 summarizes the elemental composition of HA nanoparticles, urea-modified HA nanoparticles, raw *G. sepium* and urea-modified HA nanoparticle-encapsulated *G. sepium*.

The FTIR spectrum (Figure 3d) of the encapsulated material clearly indicated that the structural integrity of urea-modified HA nanoparticles was maintained within the cavities present in *G. sepium* wood.

A slow and sustained release of N over a period more than 2 months for the two acidic soils (pH 4.2 and 5.2) and the sandy soil (pH 7) was observed (Figures 7–9).

In general, release of the nanofertilizer containing nitrogen followed a two-phase process: initial burst release, and subsequent slow and sustained release. Data indicated that the degree of the burst release correlated with the pH of the soil: $7 > 5.2 > 4.2$.

The release behaviour observed with fertilizer composition is not as uniform as that observed for drug-release compositions. This may possibly be due to fluctuations in the physical environment of the soil compared to the relatively stable physical parameters present in a biological system. Furthermore, in the presence of two different types of nanosystems in the fertilizer composition, slow-release behaviour can be expected to occur in different steps. Once the urea-modified HA nanoparticles are encapsulated within the cavities present in the wood, these cavities become reservoirs for storage of urea-modified HA nanoparticles. When the encapsulated *G. sepium* wood pieces come into contact with water in the soil, urea localized in large vascular canals would be released

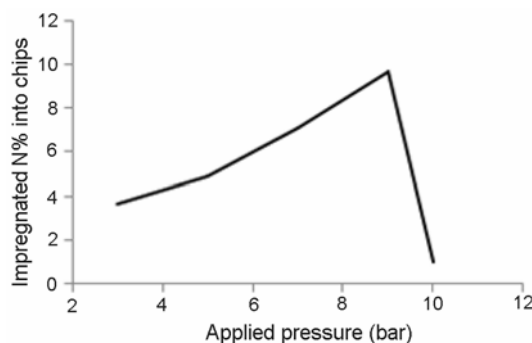


Figure 6. Impregnated N percentage at different pressure values.

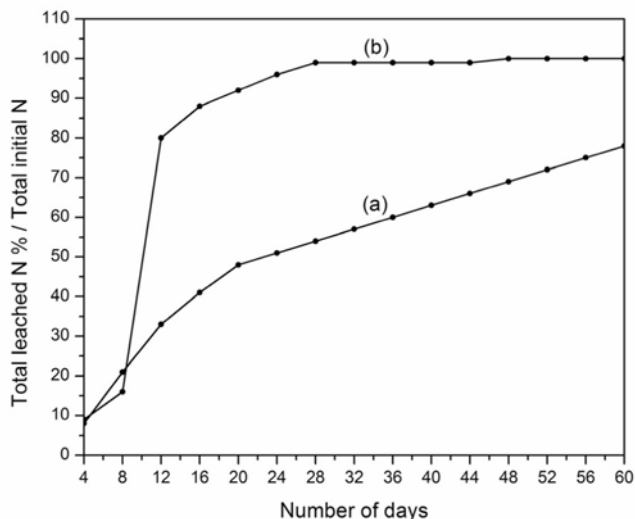


Figure 7. Nitrogen release behaviour at soil pH 4.2. (a) Urea-adsorbed HA nanoparticles encapsulated in *G. sepium*. (b) Commercial fertilizer.

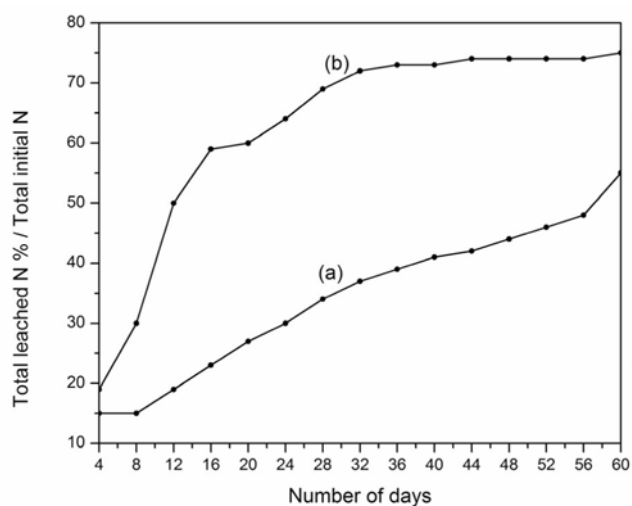


Figure 8. Nitrogen release behaviour at soil pH 5.2. (a) Urea-adsorbed HA nanoparticles encapsulated in *G. sepium*. (b) Commercial fertilizer.

early during the release process. Cells which are smaller in volume can be expected to release urea at an intermediate stage. Urea-encapsulated HA nanoparticles localized within the smaller volumes of intercellular spaces may release nitrogen at the final stages during slow-release.

The new fertilizer composition displayed more uniform release properties at pH 4.2 and 7. In general, at all pH values, even on the day 60 the nanofertilizer was releasing nitrogen > 10 mg, clearly showing the efficacy of the slow release process. On the other hand, fluctuations in the nitrogen release behaviour were observed in the funnels which contained the commercial fertilizer. This was attributed to the release of a large quantity of nitrogen

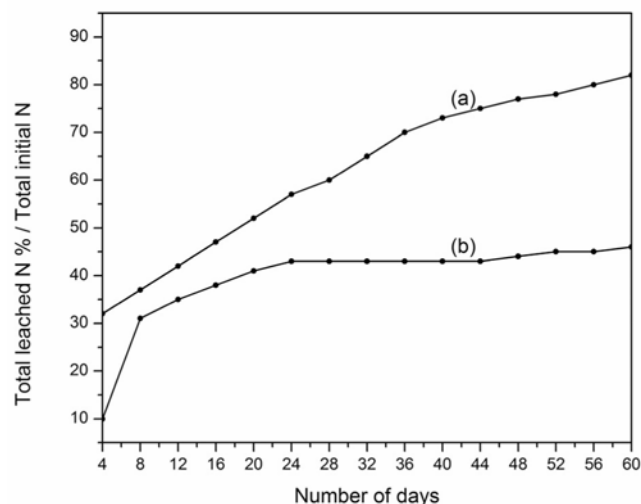


Figure 9. Nitrogen release behaviour at soil pH 7. (a) Urea adsorbed HA nanoparticles encapsulated in *G. sepium*. (b) Commercial fertilizer.

at about day 4 followed by the release of low and non-uniform quantities until around day 30, subsequently vanishing to negligible amounts mimicking the fate of conventional fertilizer formulations in the soil. Also, the commercial fertilizer which contains urea may have been lost as gaseous nitrogen. Such losses are minimized in the urea-modified nanofertilizer because it is sequestered inside the cavities of *G. sepium* wood until release. Further, when the particle size of HA reaches the nanolevel, it renders a large surface area, thus facilitating large amount of urea molecules to be attached onto the surface of the nanoparticles. The presence of strong interactions between nanoparticles and the urea molecules may have contributed significantly towards the slow and sustained release of urea when the system is encapsulated within the cell cavities.

According to the preliminary data obtained, the urea-modified nanoHA-encapsulated *G. sepium* fertilizer composition shows a significant degree of slow and sustained release of urea. Advantages of the above slow-release fertilizer would be improved efficiency and higher crop yield as the nutrients are released over time, thus enhancing hitherto problematic NUE. In addition to having an impact on energy and economy as highlighted above, the novel nanostrategy is envisaged to result in reduced environmental damage from leaching of nitrogen, compared to conventional water-soluble fertilizers.

Studies leading to dose optimization of the above nanofertilizer in the laboratory scale leading to field trials are in progress.

The urea-modified HA nanoparticle-encapsulated *G. sepium* nanocomposite displays a slow and sustained release of nitrogen over time at three different pH values. The proposed fertilizer composition may maximize the NUE while minimizing the adverse effects to the environment due to use of large quantities of fertilizer in agriculture.

1. Monreal, C. M., McGill, W. B. and Nyborg, M., Spatial heterogeneity of substrates: effects of hydrolysis, immobilization and nitrification of urea-N. *Can. J. Soil Sci.*, 1986, **66**, 499–511.
2. Hussein, M. Z., Zainal, Z., Yahaya, A. H. and Foo, D. W. V., Controlled release of a plant growth regulator, 1-naphthaleneacetate from the lamella of Zn–Al-layered double hydroxide nanocomposite. *J. Control. Release*, 2002, **82**, 417–427.
3. Sastry, R. K., Rashmi, H. B., Rao, N. H. and Ilyas, S. M., Integrating nanotechnology into agri-food systems research in India: a conceptual framework. *Technol. Forecast. Soc.*, 2010, **77**, 639–648.
4. Hossain, K. Z., Monreal, C. M. and Sayari, A., Adsorption of urease on PE-MCM-41 and its catalytic effect on hydrolysis of urea. *Colloid Surf. B*, 2008, **62**, 42–50.
5. De Rosa, M. C., Monreal, C., Schnitzer, M., Walsh, R. and Sultan, Y., Nanotechnology in fertilizers. *Nature Nanotechnol.*, 2010, **5**, 91.
6. Cao, H., Zhang, L., Zheng, H. and Wang, Z., Hydroxyapatite nanocrystals for biomedical applications. *J. Phys. Chem. C*, 2010, **114**(43), 18352–18357.
7. Teng, S. H., Lee, E. J., Wang, P., Jun, S. H., Han, C. M. and Kim, H. E., Functionally gradient chitosan/hydroxyapatite composite scaffolds for controlled drug release. *J. Biomed. Mater. Res. B*, 2008, **90**, 275–282.
8. Mateus, A. Y. P., Barrias, C. C., Ribeiro, C., Ferraz, M. P. and Monteiro, F. J., Comparative study of nanohydroxyapatite microspheres for medical applications. *J. Biomed. Mater. Res. A*, 2007, **86**, 483–493.
9. Ferraz, M. P., Mateus, A. Y., Sousa, J. C. and Monteiro, F. J., Nanohydroxyapatite microspheres as delivery system for antibiotics: release kinetics, antimicrobial activity, and interaction with osteoblasts. *J. Biomed. Mater. Res. A*, 2007, **81**, 994–1004.
10. Zhu, W. *et al.*, Experimental study on the conduction function of nano-hydroxyapatite artificial bone. *Micro Nano Lett.*, 2010, **5**, 19–27.
11. Liu, C., Biomimetic synthesis of collagen/nano-hydroxyapatite scaffold for tissue engineering. *J. Bionic Eng.*, 2008, **5**, 1–8.
12. Damien, V. and Revell, P. A., Coralline hydroxyapatite bone graft substitute: a review of experimental studies and biomedical applications. *J. Appl. Biomater. Biomech.*, 2004, **2**, 65–73.
13. Mateus, A. Y. P., Ferraz, M. P. and Monteiro, F. J., Microspheres based on hydroxyapatite nanoparticles aggregates for bone regeneration. *Key Eng. Mater.*, 2007, **330–332**, 243–246.
14. Monmaturapoj, N., Nano-size hydroxyapatite powders preparation by wet-chemical precipitation route. *J. Met. Mater. Miner.*, 2008, **18**, 15–20.
15. Han, Y., Wang, X. and Li, S., A simple route to prepare stable hydroxyapatite nanoparticles suspension. *J. Nanopart. Res.*, 2008, **11**, 1235–1240.
16. Poinern, G. E., Brundavanam, R. K., Mondinos, N. and Jiang, Z. T., Synthesis and characterization of nanohydroxyapatite using an ultrasound assisted method. *Ultrason. Sonochem.*, 2009, **16**, 469–474.
17. Nandi, S. K., Kundu, B., Ghosh, S. K., De, D. K. and Basu, D., Efficacy of nano-hydroxyapatite prepared by an aqueous solution combustion technique in healing bone defects of goat. *J. Vet. Sci.*, 2008, **9**, 83–191.
18. Manafi, S. A. and Jougehdoost, S., Synthesis of hydroxyapatite nanostructure by hydrothermal condition for biomedical application. *Iran J. Pharm.*, 2009, **5**, 89.
19. Montazeri, L., Javadpour, J., Shokrgozar, M. L., Bonakdar, S. and Javadian, S., Hydrothermal synthesis and characterization of hydroxyapatite and fluorohydroxyapatite nano-size powders. *Biomed. Mater.*, 2010, **5**, 7.
20. Chaudhry, A. A., Haque, S., Kellici, S., Boldrin, P., Rehman, I., Khalid, F. A. and Darr, J. A., Instant nano-hydroxyapatite: a continuous and rapid hydrothermal synthesis. *Chem. Commun.*, 2006, **21**, 2286.
21. Liu, D. M., Troczynski, T. and Tseng, W. J., Water-based sol-gel synthesis of hydroxyapatite: process development. *Biomaterials*, 2001, **22**, 1721–1730.
22. Cho, J. S. and Kang, Y. C., Nano-sized hydroxyapatite powders prepared by flame spray pyrolysis. *J. Alloy. Compd.*, 2008, **464**, 282–287.
23. Han, W. W. T. and Misra, R. D. K., Biomimetic chitosan–nano-hydroxyapatite composite scaffolds for bone tissue engineering. *Acta Biomater.*, 2009, **5**, 1182–1197.
24. Katti, K. S., Katti, D. R. and Dash, R., Synthesis and characterization of a novel chitosan/montmorillonite/hydroxyapatite nanocomposite for bone tissue engineering. *Biomed. Mater.*, 2008, **3**, 034122.
25. Li, J., Shu, D., Yin, J., Liu, Y., Yao, F. and Yao, V., Formation of nano-hydroxyapatite crystal *in situ* in chitosan–pectin polyelectrolyte complex network. *Mater. Sci. Eng. C*, 2010, **30**, 795–803.
26. Poursamar, S. A., Rabiee, M., Samadikuchaksaraei, V., Karimi, M. and Azami, M., Influence of the value of the pH on the preparation of nano hydroxyapatite polyvinyl alcohol composites. *J. Ceram. Process. Res.*, 2009, **10**, 679–682.
27. Mcquaire, R. G., Ching, J. Y. C., Vignaud, E., Lebugue, A. and Mann, S., Synthesis and characterization of amino acid-functionalized hydroxyapatite nanorods. *J. Mater. Chem.*, 2004, **14**, 2277–2281.

ACKNOWLEDGEMENT. We thank Sri Lanka Institute of Nanotechnology and Hayleys Agro Ltd, Sri Lanka for financial support.

Received 7 February 2011; revised accepted 19 May 2011

Long distance electrical signalling in jute plant

Prajjal Datta and P. Palit*

Plant Physiology Section, Central Research Institute for Jute and Allied Fibres, Barrackpore 700 120, India

To gain an understanding of the velocity and mechanism of electrical signalling for long-distance communication in plants, a slender jute (*Corchorus capsularis* L.) stem was provided with a train of electrical pulses through a specially designed microelectrode at the phloem region. The propagated electric signal was detected at a distance 150 cm above the input region. The applied square pulses were reduced considerably and modified to curved ones at the output point. The signal moved extracellular with a measured velocity of almost nanoseconds from input to output electrode. Several hypotheses for such rapid electrical signalling are proposed.

Keywords: Electrical signal, jute plant, long-distance communication, square and curved waves.

*For correspondence. (e-mail: palitpratip@gmail.com)